WNT1-Inducible Signaling Pathway Protein 1 Contributes to Ventilator-Induced Lung Injury

Hui-Hua Li[1], Quan Li[1,3,8], Pengyuan Liu[6], Yulin Liu[5], Jin Li[2], Karla Wasserloos[2], Wei Chao[7], Ming You[6], Tim D. Oury[4], Sodhi Chhinder[3], David J. Hackam[3], Timothy R. Billiar[3], George D. Leikauf[2], Bruce R. Pitt[2], and Li-Ming Zhang[1]

[1]Department of Anesthesiology, and [3]Department of Surgery, University of Pittsburgh School of Medicine, Pittsburgh, Pennsylvania; [2]Department of Environmental and Occupational Health, and [4]Department of Pathology, Graduate School of Public Health, University of Pittsburgh, Pittsburgh, Pennsylvania; [5]Department of Pathology and Laboratory Medicine, Allegheny General Hospital, Drexel University College of Medicine, Pittsburgh, Pennsylvania; [6]Wisconsin Cancer Center, Medical College of Wisconsin, Milwaukee, Wisconsin; [7]Department of Anesthesia, Critical Care and Pain Medicine, Massachusetts General Hospital, Harvard Medical School, Boston, Massachusetts; and [8]Department of Anesthesiology, Shanghai Tenth People's Hospital, Tongji University School of Medicine, Shanghai, China

Although strides have been made to reduce ventilator-induced lung injury (VILI), critically ill patients can vary in sensitivity to VILI, suggesting gene–environment interactions could contribute to individual susceptibility. This study sought to uncover candidate genes associated with VILI using a genome-wide approach followed by functional analysis of the leading candidate in mice. Alveolar–capillary permeability after high tidal volume (HTV) ventilation was measured in 23 mouse strains, and haplotype association mapping was performed. A locus was identified on chromosome 15 that contained ArfGAP with SH3 domain, ankyrin repeat and PH domain 1 (*Asap1*), adenylate cyclase 8 (*Adcy8*), WNT1-inducible signaling pathway protein 1 (*Wisp1*), and N-myc downstream regulated 1 (*Ndrg1*). Information from published studies guided initial assessment to *Wisp1*. After HTV, lung WISP1 protein increased in sensitive A/J mice, but was unchanged in resistant CBA/J mice. Anti-WISP1 antibody decreased HTV-induced alveolar–capillary permeability in sensitive A/J mice, and recombinant WISP1 protein increased HTV-induced alveolar–capillary permeability in resistant CBA/J mice. HTV-induced WISP1 coimmunoprecipitated with glycosylated Toll-like receptor (TLR) 4 in A/J lung homogenates. After HTV, WISP1 increased in strain-matched control lungs, but was unchanged in TLR4 gene–targeted lungs. In peritoneal macrophages from strain-matched mice, WISP1 augmented LPS-induced TNF release that was inhibited in macrophages from TLR4 or CD14 antigen gene–targeted mice, and was attenuated in macrophages from myeloid differentiation primary response gene 88 gene–targeted or TLR adaptor molecule 1 mutant mice. These findings support a role for WISP1 as an endogenous signal that acts through TLR4 signaling to increase alveolar–capillary permeability in VILI.

Keywords: genome-wide association study; acute lung injury; acute respiratory distress syndrome

CLINICAL RELEVANCE

The current study using haplotype association mapping in inbred mouse strains identified several candidate genes associated with ventilator-induced lung injury (VILI). Functional analysis demonstrated that WNT1-inducible signaling pathway protein 1 protein plays an important role in the pathogenesis of VILI in mice probably through modulating and/or amplifying Toll-like receptor 4–mediated signaling.

The incidence of acute lung injury (also known as acute respiratory distress syndrome) is ~190,000 patients per year in the United States (1). Mechanical ventilation is a component of supportive therapy in the management of acute lung injury (2), but such therapy may produce an iatrogenic complication referred to as ventilator-induced lung injury (VILI). Much of the overall reduction in mortality from acute lung injury over the years has been ascribed to limiting VILI through lung-protective mechanical ventilation strategies (3). Nonetheless, the etiology of VILI remains unclear, and the sensitivity to VILI varies in patient subpopulations, suggesting that genetic determinants may control individual susceptibility.

Previously, multiple investigators have reproduced elements of acute lung injury after high tidal volume (HTV) in experimental animals. Several approaches have been used to identify proteins that contribute to the pathogenesis of VILI in these models. In addition, microarray analysis has yielded several candidate transcripts in pathways of inflammation, innate immunity, oxidative stress, and intracellular signaling associated with VILI in rodents (4–6). Specific proteins and pathways include neutrophil elastase (7), Toll-like receptors (TLRs) (8, 9), nuclear factor (erythroid-derived 2)–like 2 (10), nitric oxide synthase 2 (11), nitric oxide synthase 3 (12), integrins (13), JNK signaling (14), and ectonucleotidases (15). Amphiregulin and other proteins have also been associated with injury in ventilated perfused mouse lung (devoid of contributions of neutrophils or other leukocytes) (4). Other investigators have noted that mouse strains differ in acute lung injury induced by various forms of high volume/pressure ventilation (16, 17). These studies were limited to a few inbred strains, but nonetheless provide a strong rationale for a systematic study of VILI in inbred mice.

Haplotype association mapping provides an approach for identifying susceptibility genes and molecular pathways that underlie a given trait (18). Advances in genome sequence analysis and high density single-nucleotide polymorphism (SNP) maps

(*Received in original form April 3, 2012 and in final form June 5, 2012*)

This work was supported by Anesthesia Seed Grant and National Institutes of Health grants HL79456 (L.M.Z.), HL65697 (B.R.P.), ES015675, HL077763, HL085655 (G.D.L.), GM50441 (T.R.B.), and GM080906 (W.C.).

Author Contributions: Study design, H.H.L., G.D.L., B.R.P., L.M.Z.; experimental performance and acquisition of data, H.H.L., Q.L., J.L., K.W., S.C., L.M.Z.; data interpretation and statistical analysis, H.H.L., L.M.Z.; haplotype association analysis, P.L., M.Y., G.D.L., H.H.L.; tissue preparation and histology evaluation, Y.L., T.D.O.; intellectual contribution and supervision, W.C., T.R.B., D.J.H., G.D.L., B.R.P.; manuscript writing, H.H.L., G.D.L., B.R.P., L.M.Z. All coauthors have read and approved the final version for submission.

Correspondence and requests for reprints should be addressed to Li-Ming Zhang, M.D., Department of Anesthesiology, University of Pittsburgh School of Medicine, 200 Lothrop Street, MUH N467, Pittsburgh, PA 15213. E-mail: zhangl1@anes.upmc.edu

This article has an online supplement, which is accessible from this issue's table of contents at www.atsjournals.org

Am J Respir Cell Mol Biol Vol 47, Iss. 4, pp 528–535, Oct 2012

Originally Published in Press as DOI: 10.1165/rcmb.2012-0127OC on June 14, 2012
Internet address: www.atsjournals.org

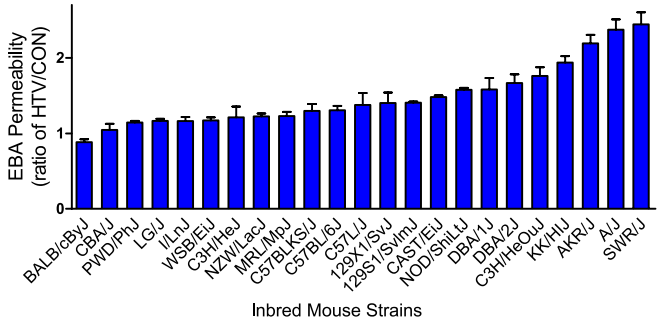

Figure 1. Ratio of Evan's blue albumin (EBA) permeability in high tidal volume (HTV) ventilated mice compared with spontaneous breathing control (CON) mice in 23 mouse strains. EBA permeability index was calculated by dividing the pulmonary tissue EBA at 620 nm absorbance per gram of lung tissue by the plasma EBA at 620 nm absorbance. EBA permeability in each strain was normalized as permeability ratio of HTV mice to CON mice. Values are means (±SEM); $n = 216$ mice, four to six mice per mouse strain in each CON and HTV group.

have facilitated our ability to identify genetic determinants of complex traits in mice. Its relevance to human pathophysiology is apparent in that 99% of mouse genes have homologs in humans, 96% are in syntenic locations, and many genetic alterations identified in mouse models have a common genetic equivalent (or ortholog) in humans (19). In the present study, we quantified changes in alveolar–capillary permeability with Evan's blue albumin (EBA) after HTV ventilation (20 ml/kg × 4 h) in 23 inbred mouse strains and performed haplotype association mapping to identify genes with significant SNP association with VILI.

MATERIALS AND METHODS

Experimental animal protocols were performed in accordance with guidelines approved by the Institutional Animal Care and Use Committee at the University of Pittsburgh (Pittsburgh, PA). Inbred mice (female, 8–12 wk) used for haplotype association mapping were purchased from The Jackson Laboratory (Bar Harbor, ME). A genetically diverse panel of 23 mouse strains was phenotyped, and haplotype association mapping was performed as described previously (20). VILI-induced alveolar capillary permeability of EBA was measured as described previously (9). Briefly, anesthetized mice were ventilated with HTV (20 ml/kg body weight × 100 breaths/min × 4 h; 0 positive end-expiratory pressure). Another group of strain-matched control mice (CON) underwent tracheotomy, but breathed spontaneously for 4 hours. Previously, we noted no significant difference in alveolar–capillary permeability between low tidal volume ventilation (7 ml/kg body weight) and spontaneous breathing. After HTV or spontaneous breathing, A/J mouse lungs were homogenized in immunoprecipitation lysis/wash buffer (Pierce, Rockford, IL) with complete mini-protease inhibitors (Roche, Mannheim, Germany). Coimmunoprecipitation was performed with an affinity-purified anti–WNT1 inducible signaling pathway protein (WISP) 1 antibody (R&D Systems, Minneapolis, MN) or anti–TLR4–MD2 antibody (BD Pharmingen, San Diego, CA). To examine the contribution of specific TLR signaling proteins, TNF release was measured after LPS with or without WISP1 protein from peritoneal macrophages obtained from gene-targeted mice, including mice deficient in TLR4 ($TLR4^{-/-}$) (21), myeloid differentiation primary response gene (MyD) 88 ($MyD88^{-/-}$) (22), and CD14 antigen ($CD14^{-/-}$) (23). In addition, peritoneal macrophages from TLR adaptor molecule 1 (a.k.a., TRIF) ($TRIF^{-/-}$) mutant mice were used (24). Responses of macrophages from these mice were contrasted with responses of peritoneal macrophage from strain-matched (C57BL/6J) mice. Peritoneal macrophages were obtained with PBS containing 5 mM EDTA (Sigma-Aldrich, St. Louis, MO), seeded in 96-well plates at a density of 6×10^4/well, and treated with LPS with or without WISP1 protein in reduced serum OPTI-MEM medium (Invitrogen Life Technologies, Carlsbad, CA) (22 h; 5% CO_2; 37°C). Culture medium was collected and TNF levels were measured by

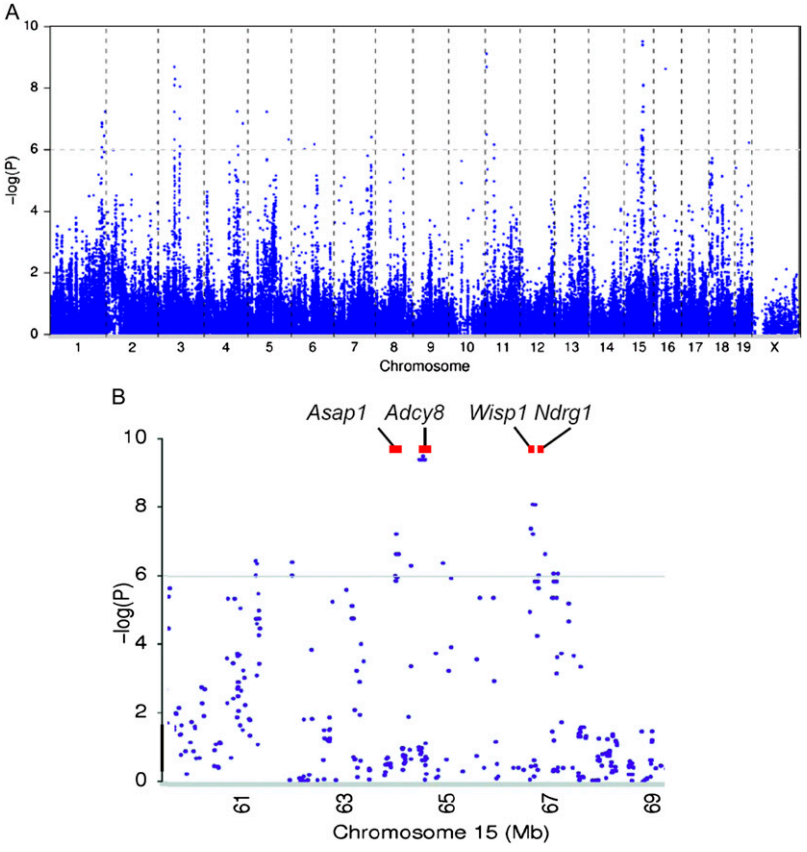

Figure 2. Haplotype association mapping of ventilator-induced lung injury (VILI) using single-nucleotide polymorphisms (SNPs) in mice. (*A*) Haplotype association map for VILI in mice. The scatter (Manhattan) plot of corresponding −log (P) association probability (*ordinate*) for each SNP at the indicated chromosomal location (*abscissa*). The *horizontal dashed line* indicates the significance level of −log (P). (*B*) Candidate genes on mouse chromosome 15 associated with VILI. Genes with one or more significant SNPs (−log (P) > 6.0) included ArfGAP with SH3 domain, ankyrin repeat and PH domain 1 (*Asap1*), adenylate cyclase 8 (*Adcy8*), WNT1-inducible signaling pathway protein 1 (*Wisp1*), and N-myc downstream regulated 1 (*Ndrg1*).

ELISA kit (R&D Systems, Minneapolis, MN). Data are means (±SEM). Statistically significant differences ($P < 0.05$, $P < 0.01$, $P < 0.001$) were determined by two-way or one-way ANOVA, followed by Bonferroni's multiple comparisons or Tukey's post test, respectively, using Graphpad Prism ver. 5.0 (GraphPad Software, San Diego, CA). Further details on the methods are presented in the supplemental material.

RESULTS

Haplotype Association Mapping of SNPs Associated with VILI in Inbred Mouse Strains

Because structural impairment in the alveolar–capillary membrane barrier, with subsequent increased pulmonary vascular permeability, is a prominent feature of acute lung injury, we used the ratio of EBA levels after HTV to EBA levels after spontaneous breathing as a quantitative trait to discriminate lung injury after mechanical ventilation in each mouse strain. The EBA permeability ratio after HTV varied roughly 2-fold among the 23 mouse strains tested (Figure 1). The resulting phenotypes were used for haplotype association mapping (Figure 2), and 33 SNP associations were linked to VILI ($-\log(P) = 6.0–9.5$) that resided within 18 genes (Table 1). Four genes, ArfGAP with SH3 domain, ankyrin repeat and PH domain 1 (*Asap1*), adenylate cyclase 8 (*Adcy8*), *Wisp1*, and N-myc downstream regulated 1 (*Ndrg1*), were located in a single region (64.1–66.7 Mbp) on chromosome 15 (Figure 2). Haplotype association mapping identifies SNP associations in linkage with functional SNPs (25); therefore, we evaluated the potential functional SNPs in these 18 candidate genes using the next generation sequencing map in various strains of mice (26).

We identified SNPs that would lead to amino acid substitution in a functional domain of the corresponding protein or alter putative transcription factor binding site in the 5′ untranslated region (UTR) of the gene. From these SNPs, we selected SNPs that had >10% minor allele frequency that could account for >10% of the phenotypic difference between the most disparate strains (*see* Table E1 in the online supplement). This approach identified nine genes. Three genes, human immunodeficiency virus type I enhancer binding protein 3 (*Hivep3*), contactin-associated protein-like 2 (*Cntnap2*), and heparan sulfate (glucosamine) 3-O-sulfotransferase 4 (*Hs3st4*), had one or more nonsynonymous SNPs in a functional domain. The other six genes, including *Wisp1* and *Ndrg1*, had one or more SNPs in the 5′ UTR that could alter a putative transcription factor binding site.

TABLE 1. SIGNIFICANT SINGLE-NUCLEOTIDE POLYMORPHISMS IDENTIFIED BY HAPLOTYPE ASSOCIATION MAPPING OF VENTILATOR-INDUCED LUNG INJURY IN MICE

Chromosome	Position	dbSNP	Region	Alleles	−log (P)	Symbol
1	181141730	rs32601567	Intron	C/T	6.75	*Smyd3*
1	181145346	rs31517246	Intron	A/G	6.08	*Smyd3*
1	181167686	rs32357487	Intron	A/G	6.75	*Smyd3*
1	181254194	rs32370428	Intron	C/T	6.75	*Smyd3*
1	181254863	rs32390461	Intron	A/G	6.75	*Smyd3*
1	181330284	rs13476264	Intron	C/T	6.87	*Smyd3*
1	181970809	rs32668729	Intron	C/T	6.84	*Cdc42bpa*
1	189141678	rs31931745	Intron	A/G	6.45	*Gpatch2*
3	75255647	rs13477201	Coding	C/T	7.01	*Wdr49*
4	119751327	rs6401898	Intron	A/G	6.12	*Hivep3*
5	65197908	rs33714346	Intron	C/T	7.23	*Klf3*
5	142665148	rs33587040	Intron	A/G	6.34	*Sdk1*
6	45945581	rs30354170	Intron	C/T	6.02	*Cntnap2*
7	131322893	rs31985864	Intron	C/T	6.41	*Hs3st4*
11	4442382	rs29417270	Intron	A/G	9.12	*Mtmr3*
11	4447839	rs26938982	Intron	A/C	8.69	*Mtmr3*
11	4470221	rs26923056	Intron	A/G	8.69	*Mtmr3*
11	4552514	rs29438722	Intron	A/T	6.50	*Ascc2*
11	30780223	rs13467861	3′ UTR	A/T	6.17	*Psme4*
15	64110550	rs31110351	Intron	C/G	6.02	*Asap1*
15	64129266	rs6177246	Intron	A/T	7.23	*Asap1*
15	64129349	rs6177728	Intron	C/T	6.64	*Asap1*
15	64169932	rs31589408	Intron	A/C	6.64	*Asap1*
15	64579156	rs31127725	Intron	C/G	9.40	*Adcy8*
15	64579327	rs31127727	Intron	C/T	9.40	*Adcy8*
15	64624571	rs31131314	Intron	A/G	9.40	*Adcy8*
15	64646875	rs13482616	Coding	C/T	9.51	*Adcy8*
15	64685909	rs32478823	Intron	A/T	9.40	*Adcy8*
15	66752215	rs13482623	3′ UTR	C/T	7.39	*Wisp1*
15	66791317	rs31744623	Intron	C/G	8.10	*Ndrg1*
15	66792183	rs31588658	Intron	A/G	7.23	*Ndrg1*
16	41868185	rs4178707	Intron	C/T	8.62	*Lsamp*
19	50686324	rs30420148	Intron	C/T	6.23	*Sorcs1*

Definition of abbreviations: Adcy8, Adenylate cyclase 8; *Asap1*, ArfGAP with SH3 domain, ankyrin repeat and PH domain 1; *Ascc2*, activating signal cointegrator 1 complex subunit 2; *Cdc42bpa*, CDC42 binding protein kinase alpha; *Cntnap2*, contactin associated protein-like 2; dbSNP, National Center for Biotechnology Information single-nucleotide polymorphism identification number; *Gpatch2*, G patch domain containing 2; *Hivep3*, human immunodeficiency virus type I enhancer binding protein 3; *Hs3st4*, heparan sulfate (glucosamine) 3-O-sulfotransferase 4; *Klf3*, Kruppel-like factor 3 (basic); −log(P), negative log of the probability; *Lsamp*, limbic system-associated membrane protein; *Mtmr3*, myotubularin related protein 3; *Ndrg1*, N-myc downstream regulated gene 1; Position, basepair location of gene; *Psme4*, proteasome (prosome; macropain) activator subunit 4; *Sdk1*, sidekick homolog 1 (chicken); *Smyd3*, SET and MYND domain containing 3; *Sorcs1*, Sortilin-related VPS10 domain containing receptor 3; UTR, untranslated region; *Wdr49*, WD repeat domain 49; *Wisp1*, WNT1-inducible signaling pathway protein 1.

Comparison of Sensitive (A/J) and Resistant (CBA/J) Mice to HTV

HTV increased EBA permeability in the sensitive A/J mouse strain compared with spontaneously breathing control (CON) after 4 hours, whereas HTV did not increase EBA permeability in the resistant CBA/J mouse strain (Figure 3A). Similarly, protein content (Figure 3B), total cell count (Figure 3C), neutrophils (Figure 3D), and macrophages (Figure 3E) in bronchoalveolar lavage (BAL) fluid increased more in sensitive A/J mice than in resistant CBA/J mice after 4 hours of HTV.

We initiated an assessment of the candidate genes on chromosome 15 based on biological plausibility, including possible functional significance in VILI and transcript expression in the mouse lung. *Wisp1* appears to be a leading candidate among the identified genes of causing VILI because: (*1*) WNT/β-catenin signaling has previously been associated with lung injury (27–30); (*2*) *Wisp1* mRNA increased in alveolar epithelia after mechanical stretch (31); and (*3*) *Wisp1* has been associated with pulmonary fibrosis in mice (32).

WISP1 protein increased markedly in lungs after HTV in the sensitive A/J mouse strain as compared with the resistant CBA/J mouse strain (Figure 4A). In addition, WISP1 protein was detected in airway and alveolar epithelium and alveolar macrophages in A/J mice exposed to spontaneous breathing control (Figure 4B), and similar localization was also found in A/J mice after HTV and resistant CBA/J mice after CON and HTV (data not shown). Immunoreactive WISP1 protein was apparent in primary alveolar macrophages obtained from either the A/J or CBA/J mouse strain (Figure 4C), but increased only in the sensitive A/J mouse strain in alveolar macrophages obtained after HTV (Figure 4D). Immunoreactive WISP1 was also present in BAL fluid (Figure 4E), suggesting that it can be secreted and act as an extracellular molecule. Similar to lung homogenate, WISP1 protein was elevated in BAL fluid of the sensitive, but not the resistant, mouse strain at 4 hours after HTV.

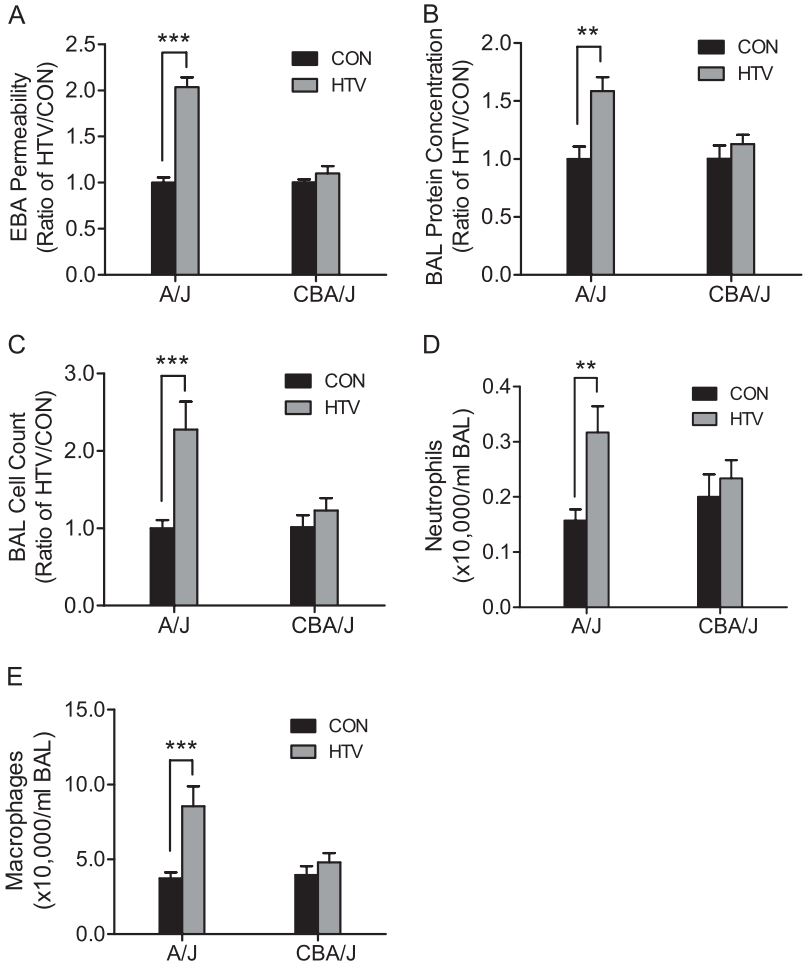

Figure 3. Lung injury increased in sensitive A/J mice after HTV ventilation as compared with resistant CBA/J mice. (*A*) EBA permeability increased in sensitive A/J mice compared with CON, whereas HTV did not increase EBA permeability in resistant CBA/J mice after 4 hours of mechanical ventilation. Values are means (±SEM) (four to six mice/group). (*B*) HTV increased bronchoalveolar lavage (BAL) protein concentration in sensitive A/J mice, whereas it failed to increase BAL protein concentration in resistant CBA/J mice after exposing them to 4 hours of mechanical ventilation compared with CON. Values are means (±SEM) (four to six mice/group). (*C*) HTV increased BAL total cell number counts in sensitive A/J mice compared with CON after 4 hours, whereas HTV did not increase BAL total cell number counts in resistant CBA/J mice. (*D*) HTV increased BAL neutrophils in sensitive A/J mice compared with CON after 4 hours, whereas HTV did not increase BAL neutrophil counts in resistant CBA/J mice. (*E*) HTV increased BAL macrophages in sensitive A/J mice after 4 hours of HTV compared with CON. Values are means (±SEM) (four to six mice/group). Significant difference from control (**$P < 0.01$, ***$P < 0.001$), as determined by two-way ANOVA followed by Bonferroni's multiple comparisons.

Reversal of Phenotype to VILI via WISP1 in Mice

Sensitive A/J mice were administered anti-WISP1 monoclonal antibody or serum IgG (0.5 μg/g in 50 μl intratracheal instillation) before HTV. Anti-WISP1 monoclonal antibody inhibited HTV-induced EBA increase in sensitive A/J mice, whereas serum IgG did not affect lung injury after HTV (Figure 5A). Resistant CBA/J mice were administered recombinant mouse WISP1 (rmWISP1) protein (0.5 μg/g in 50 μl intratracheal instillation) or PBS (50 μl intratracheal instillation) before HTV or spontaneous breathing control. rmWISP1 increased HTV-induced EBA permeability in resistant CBA/J mice, whereas PBS did not affect lung injury after HTV (Figure 5B).

WISP1 Contributes to VILI via TLR4 Signaling

Because WISP1 appears to be a critical link between mechanical stretch and innate immunity in airway epithelium (31), and TLR4 appears to be important in VILI (8, 9, 33), we assessed the relationship between WISP1 and TLR4 in VILI. TLR4 was readily detectable in A/J mouse lung, and glycosylated TLR4 (120 kD) slightly increased after 4 hours of HTV (Figure 6A). In coimmunoprecipitation assays with anti-WISP1 antibody or anti–TLR4-MD2 antibody, total WISP1 increased and coprecipitated with glycosylated TLR4 after 4 hours of HTV (Figure 6A and 6B). TLR4 gene–targeted ($TLR4^{-/-}$) mice were tested to pursue this association further. We initially confirmed that $TLR4^{-/-}$ mice were resistant to HTV-induced lung injury (Figure 7A) (8, 33), and we further found that lung WISP1 protein increased after HTV in $TLR4^{+/+}$ mice, but not in $TLR4^{-/-}$ mice, in lung tissue homogenates (Figure 7B). In peritoneal macrophages from strain-matched mice, rmWISP1 augmented LPS-induced TNF release that was inhibited in peritoneal macrophages from $TLR4^{-/-}$ or $CD14^{-/-}$ mice, and was attenuated in peritoneal macrophages from $MyD88^{-/-}$ or $TRIF^{-/-}$ mice (Figure 7C).

DISCUSSION

In this study, inbred mouse strains were found to vary roughly 2-fold in sensitivity to HTV, as manifested by increased EBA permeability. We chose to contrast HTV to spontaneously breathing mice, as we previously noted (9) that low tidal volume ventilation (7 ml/kg, 140 breaths/min) resulted in similar EBA permeability, as was determined in spontaneously breathing animals. The use of spontaneous breathing as a control also reduced the time of phenotyping and the number of mice to be tested. Using 23 mouse strains ($n = 216$ mice), haplotype association mapping yielded 18 genes with significant SNPs ($-\log$ (P) = 6.0–9.5) that associated with VILI (Table 1).

Of these 18 genes, four (*Asap1*, *Adcy8*, *Wisp1*, and *Ndrg1*) were located in a single region (64.1–66.7 Mbp) on chromosome 15 (Figure 2B). Proteins derived from these genes are associated with cell–cell focal adhesion (34), GTP-mediated cell signaling (35), WNT/β-catenin–mediated cell signaling (36), and p53-mediated caspase activation (37), respectively. It is noteworthy that none of these genes that emerged from our approach were previously noted as candidate genes for VILI.

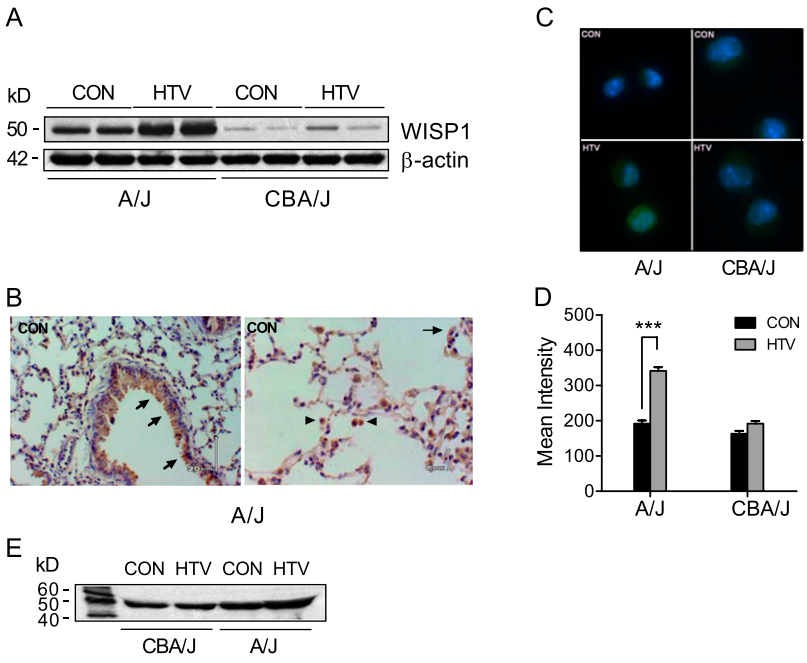

Figure 4. Mechanical ventilation increased WISP1 protein in sensitive A/J mice. (*A*) HTV ventilation increased WISP1 protein level in lung tissues determined by immunoblot in sensitive A/J mice, whereas there was no change in WISP1 levels in resistant CBA/J mice exposed to 4 hours of HTV. β-actin was the loading control. Data are representative of three tests. (*B*) Immunohistochemistry of WISP1 protein in CON mice from the sensitive A/J strain. The localization of WISP1 protein was similarly detected in airway and alveolar epithelium (*arrow*) and alveolar macrophages (*arrowhead*) in both sensitive A/J and resistant CBA/J strains after CON and HTV. Data shown are representative of two tests. (*C*) Immunofluorescence staining for WISP1 protein (Alexa-488 fluorescently labeled antibody, *green color*) in alveolar macrophages increased more in sensitive A/J mice than in resistant CBA/J mice after HTV. (*D*) The mean fluorescence intensity for WISP1 immunostaining was determined by quantifying fluorescent intensity of 10–20 cells in 4–5 fields that were randomly selected with Nikon image software NIS-Element AR 3.2. Values are means (±SEM). Significant difference from control (***$P < 0.001$), as determined by two-way ANOVA followed by Bonferroni's multiple comparisons. (*E*) Immunoblot of WISP1 protein in BAL fluid was elevated after 4 hours of HTV in the sensitive A/J strain compared with the resistant CBA/J strain.

To prioritize among these candidate genes, we evaluated whether each gene had tissue-specific expression (e.g., mRNA/protein expressed in mouse lung), was relevant to VILI (e.g., reasonable, functional role critical to barrier function), or genetic variation with possible functional significance in VILI (e.g., polymorphisms exist that produce gain- or loss-of-function). This approach is reminiscent of the decision plan in prioritizing data from microarray analysis of interstitial pulmonary fibrosis in which *Wisp1* emerged as a leading candidate for Königshoff and colleagues (32).

Assessment of SNPs in *Wisp1* revealed potential functional SNPs within the 5′ UTR that would cause the loss of transcription factor CP (TFCP) 2 (a.k.a., LBP-1 or LSF) that could account for 45% of the phenotypic differences between the polar strains. In addition, three SNPs (rs35244636, rs116716037, and rs113859079) present in the human WISP1 promoter could alter putative transcription factor binding site, and rs35244636 also could result in the loss of a predicted TFCP2 binding site. Previous studies indicate that TFCP2 can be activated by secreted phosphoprotein 1 (38), activates fibronectin promoter upon epithelial–mesenchymal transition (EMT) induction by snail homolog 1 (Snail1) (39), and enhances angiogenesis by transcriptional activation of matrix metalloproteinase 9 (40) that modulates matrix turnover and inflammation in VILI (41, 42). Accordingly, we pursued WISP1 protein in further detail in the current study on VILI in mice.

A CCN family (a family of secreted cysteine-rich growth regulators named as an abbreviation derived from designations of the main members: CYR61, CTGF, and NOV) protein, WISP1 contains four conserved cysteine-rich domains: insulin-like growth factor–binding domain, von Willebrand factor type C module, thrombospondin domain, and C-terminal cysteine knot-like domain (43). WISP1 is a secreted matricellular protein that has been associated with cell proliferation, differentiation, and extracellular matrix deposition and turnover (36). As a target gene in WNT/β-catenin signaling, Königshoff and colleagues (32) reported that WISP1 mRNA increased in bleomycin-induced pulmonary fibrosis. In addition, neutralizing WISP1 antibody attenuated pulmonary fibrosis (decreased lung collagen), improved lung function (increased lung compliance), and increased survival in mice. In cell culture, recombinant WISP1 protein increased proliferation and EMT in mouse primary cultured type II cells and enhanced deposition of extracellular matrix proteins in murine and human lung fibroblasts. In addition, activation of WNT/β-catenin pathway in bleomycin-induced fibrosis in mice was confirmed with Tcf-Optimal

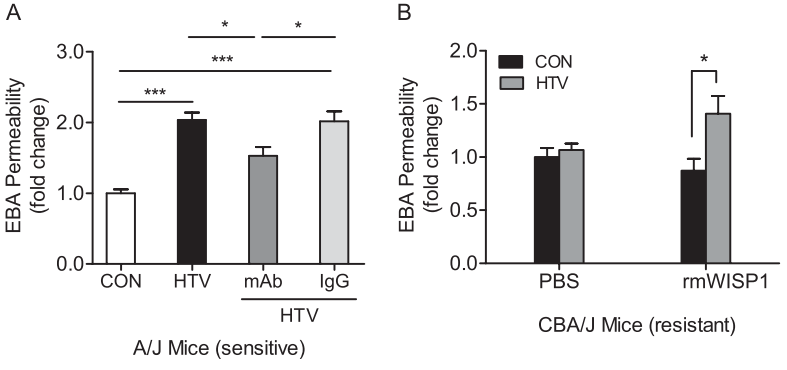

Figure 5. Anti-WISP1 monoclonal antibody (mAb) or recombinant mouse WISP1 protein (rmWISP1) reversed phenotype to VILI in sensitive A/J mice or resistant CBA/J mice, respectively. (*A*) A/J mice were intratracheally administered anti-WISP1 mAb or serum IgG (0.5 μg/g in 50 μl PBS) using a MicroSpray syringe before HTV mechanical ventilation. Lung injury was evaluated by measuring EBA permeability after 4 hours of HTV or CON. Anti-WISP1 mAb decreased EBA permeability after 4 hours of HTV-induced lung injury in sensitive A/J mice, whereas serum IgG did not decrease lung injury. Values are means (±SEM) (four to six mice/group). Significant difference from control (*$P < 0.05$, ***$P < 0.001$), as determined by one-way ANOVA followed by Tukey's post test. (*B*) CBA/J mice were intratracheally instilled with rmWISP1 (0.5 μg/g in 50 μl PBS) or 50 μl PBS as a control using a MicroSpray syringe before HTV mechanical ventilation or CON. Values are means (±SEM) (n = four to six mice/group). Significant difference from control (*$P < 0.05$), as determined by two-way ANOVA followed by Bonferroni's multiple comparisons.

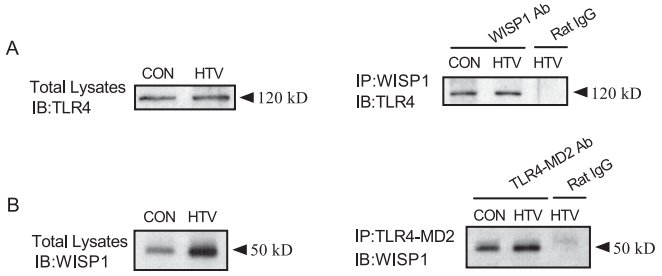

Figure 6. WISP1 interacted with Toll-like receptor (TLR) 4 in VILI. A/J mouse lung tissues obtained from 4-hour CON or HTV mechanical ventilation were homogenized and total lysates were immunoprecipitated (IP) with anti-WISP1 antibody or anti–TLR4–MD2 antibody before immunoblot (IB) was performed. (*A*) Glycosylated form of TLR4 (120 kD) was detected with anti-TLR4 antibody (IB: TLR4) either in the whole lung tissue lysates (Total Lysates) or after immunoprecipitation with anti-WISP1 antibody (IP: WISP1). (*B*) WISP1 was detected with anti-WISP1 antibody (IB: WISP1) either in the whole lung tissue lysates (Total Lysates) or after immunoprecipitation with anti–TLR4–MD2 antibody (IP: TLR4-MD2). Antibody species-matched serum (Rat IgG) was used as a negative control for coprecipitation experiments. Results are representative of tests performed on three occasions.

Promoter β-Galactosidase (TOPGAL) reporter mice, and localization to alveolar type II cells was confirmed by immunohistochemistry, including expression of important WNT/β-catenin target molecules in addition to WISP1. These and other observations in this comprehensive study clearly delineate the potential importance of WISP1 in injury and repair of airway epithelium.

The importance of WNT/β-catenin signaling in VILI was put forth by Slutsky and colleagues (27, 28), who have proposed a role of this pathway and EMT in VILI and subsequent pulmonary fibrosis (44). In addition, Heise and colleagues (31) reported that WISP1 mRNA increased in mechanically stretched mouse alveolar type II cells, and that stretch-induced decreases in epithelial cadherin 1 and increases in vimentin and actin transcript levels were prevented in cells treated with WISP1 antibody. Accordingly, activation of WNT/β-catenin signaling and one of its target genes, *Wisp1*, in airway epithelium is an early and important part of lung injury and repair, including the response to mechanical stretch.

In our study, we found that WISP1 protein in the lung and the BAL fluid increased in sensitive A/J mice, but not in resistant CBA/J mice, after HTV (Figure 4). Interestingly, the identified potential functional SNP in proximal promoter in the *Wisp1* gene may account for the differential expression of WISP1 protein level in the sensitive A/J strain and resistant CBA/J strain. Moreover, the strategy of using either WISP1 antibody in sensitive A/J mice or recombinant WISP1 protein in resistant CBA/J mice successfully reversed the strain-specific response to VILI, thereby supporting a functional role of WISP1 protein in VILI. Collectively, these findings suggest that, as a secreted protein, WISP1 plays an important role in the pathogenesis of VILI in mice.

TLRs play a pivotal role in the innate immune response in sensing and responding to cellular injury in the lung (45). TLR4 has been associated with VILI in animal models (8, 9, 33). Previously, we reported that the TLR4–MyD88 signaling pathway is critical to VILI in mice in that lung TLR4 increased and led to reduced "anti-inflammatory" IκBα, suggesting that increased TLR4 accounts for the increased inflammatory response (9). Furthermore, the demonstration that innate immunity transduces mechanical stress responses via WNT/β-catenin pathway in alveolar epithelial cells (31) prompted us to pursue such interconnections between WISP1, TLR4, and VILI. We confirmed that TLR4 gene–targeted mice ($TLR4^{-/-}$), compared with strain-matched control ($TLR4^{+/+}$), lack an increase in HTV-induced EBA permeability (Figure 7A). We also found that $TLR4^{-/-}$ mice did not have increased WISP1 protein after 4 hours of HTV (Figure 7B).

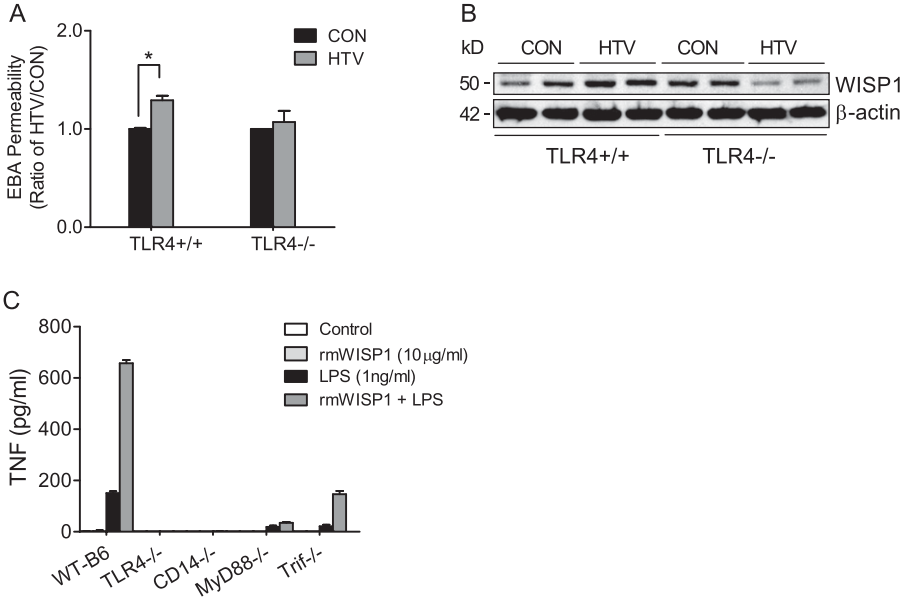

Figure 7. WISP1 contribution to VILI is dependent on TLR4 signaling pathway. (*A*) HTV increased EBA permeability in $TLR4^{+/+}$ mice compared with CON, but did not increase EBA permeability in $TLR4^{-/-}$ mice after 4 hours of mechanical ventilation. Values are means (±SEM) ($n = 3$ mice/group). Significant difference from control (*$P < 0.05$), as determined by two-way ANOVA followed by Bonferroni's multiple comparisons. (*B*) WISP1 protein expression was determined in strain-matched control ($TLR4^{+/+}$) and TLR4 gene–targeted ($TLR4^{-/-}$) mice after 4 hours of HTV ventilation. HTV increased WISP1 protein expression in $TLR4^{+/+}$ mice, but not in $TLR4^{-/-}$ mice compared with CON. β-actin was the loading control. Data are representative of three tests. (*C*) rmWISP1 enhanced LPS-induced TNF release in peritoneal macrophages via CD14–TLR4 signaling. Peritoneal macrophages were seeded in 96-well plates at a density of 6×10^4 cells/well for 24 hours before treating with indicated concentrations of rmWISP1, LPS, and LPS + rmWISP1 for 22 hours, and TNF release in the culture medium was measured by ELISA. rmWISP1, by itself, caused minimal TNF release. rmWISP1, however, enhanced LPS-induced TNF release in peritoneal macrophages from C57BL/6J strain-matched control (WT-B6), but did not amplify LPS-induced TNF release in macrophages obtained from TLR4 gene–targeted ($TLR4^{-/-}$) mice or CD14 gene–targeted ($CD14^{-/-}$) mice. In addition, rmWISP1-enhanced LPS-induced TNF release was inhibited more in macrophages isolated from myeloid differentiation primary response gene 88 gene–targeted ($MyD88^{-/-}$) mice than in macrophages from TLR adaptor molecule 1 (TICAM1; a.k.a., TRIF) mutant ($TRIF^{-/-}$) mice. Values are means (±SEM) from three independent experiments in duplicate wells.

In the current study, we also found that glycosylated TLR4 (120 kD) increased, and, more importantly, we demonstrated for the first time that WISP1 coimmunoprecipitated with the TLR4–MD2 complex in sensitive A/J mouse lung after HTV-induced injury, indicating a physical interaction between WISP1 and TLR4 (Figure 6). The glycosylation of TLR4 and MD2 is essential in maintaining functional TLR4 signaling (46). In addition, WISP1 is capable of binding directly with other extracellular matrix proteoglycans, including biglycan and decorin (47). Small leucine-rich proteoglycans, biglycan and decorin, can act as powerful damage-associated molecular pattern moleclues (DAMPs) after proteolytic release from the extracellular matrix, and are expressed in the lung during lung injury (48, 49).

To test the possible consequence to cell signaling of the WISP1 and TLR4 interaction, we further examined the effect of recombinant WISP1 protein on cytokine release in primary cultures of mouse peritoneal macrophages. rmWISP1, by itself, did not cause a measureable increase in TNF release in primary macrophages, but it was capable of enhancing TNF release from $TLR4^{+/+}$ primary macrophages in the presence of the prototypic TLR4 agonist, LPS. This enhanced effect of rmWISP1 on LPS-induced TNF release was not likely due to endotoxin contamination within rmWISP1, as levels of the latter ($\leqslant$37 pg/ml LPS) were below that required (100 pg/ml) to activate cultured peritoneal macrophages in our laboratory and those of others (50). In addition, although LPS-stimulated TNF release by macrophages was totally inhibited by polymyxin B treatment, the amplified effect of rmWISP1 on TNF release in primary macrophages, combined with other TLR agonists or another DAMP, high-mobility group box-1 protein, was present even after polymyxin B treatment (unpublished data).

The effect of rmWISP1 on LPS-induced TNF release was inhibited in macrophages isolated from $TLR4^{-/-}$ or $CD14^{-/-}$ gene–targeted mice. This effect was decreased more in macrophages from the innate immune adaptor molecule $MyD88^{-/-}$ gene–targeted mice than in macrophages from another innate immune adaptor molecule, $TRIF^{-/-}$ mutant mice (Figure 7C), suggesting that the enhanced effect of WISP1 with LPS is TLR4 and CD14 dependent, and is probably more likely mediated through TLR4–MyD88 signaling than through TLR4–TRIF signaling.

Although we did not detect an effect of rmWISP1 alone on inflammatory cytokine release in primary macrophages *in vitro*, this is probably due to lack of cofactors likely to be present *in situ* in lung injury. WISP1 increased alveolar–capillary permeability *in vivo* (Figure 5B) and magnified the effect of TLR4 agonist *in vitro* (Figure 7C) with its physical interaction with TLR4 (Figure 6), suggesting that WISP1, as a secreted protein, may be released from epithelial cells and activated alveolar macrophages within the extracellular matrix under HTV mechanical stress. This supports WISP1 as an adaptor protein that binds and presents cofactors (perhaps DAMPs or LPS itself) to CD14 to activate TLR4 signaling in macrophages and modulate or amplify a robust inflammatory response in an autocrine and paracrine fashion, resulting in inflammation and pulmonary edema (VILI).

In summary, the current study demonstrates that WISP1, identified by a genome-wide approach, acts as an adjuvant adaptor molecule that contributes to VILI in mice, probably through modulating and/or amplifying TLR4-mediated cellular functions. The association of WISP1 with TLR4 is 2-fold, and includes both the increased WISP1 levels in HTV and activation of TLR4 signaling, leading to further lung injury. Modulation of both TLR4 and WNT/β-catenin signaling may provide novel preventive (e.g., used as a biomarker) and therapeutic strategies in VILI in the future.

Author disclosures are available with the text of this article at www.atsjournals.org.

References

1. Rubenfeld GD, Caldwell E, Peabody E, Weaver J, Martin DP, Neff M, Stern EJ, Hudson LD. Incidence and outcomes of acute lung injury. *N Engl J Med* 2005;353:1685–1693.
2. Wheeler AP, Bernard GR. Acute lung injury and the acute respiratory distress syndrome: a clinical review. *Lancet* 2007;369:1553–1564.
3. Matthay MA, Zimmerman GA. Acute lung injury and the acute respiratory distress syndrome: four decades of inquiry into pathogenesis and rational management. *Am J Respir Cell Mol Biol* 2005;33:319–327.
4. Dolinay T, Kaminski N, Felgendreher M, Kim HP, Reynolds P, Watkins SC, Karp D, Uhlig S, Choi AM. Gene expression profiling of target genes in ventilator-induced lung injury. *Physiol Genomics* 2006;26:68–75.
5. Ma SF, Grigoryev DN, Taylor AD, Nonas S, Sammani S, Ye SQ, Garcia JG. Bioinformatic identification of novel early stress response genes in rodent models of lung injury. *Am J Physiol Lung Cell Mol Physiol* 2005;289:L468–L477.
6. Wurfel MM. Microarray-based analysis of ventilator-induced lung injury. *Proc Am Thorac Soc* 2007;4:77–84.
7. Kaynar AM, Houghton AM, Lum EH, Pitt BR, Shapiro SD. Neutrophil elastase is needed for neutrophil emigration into lungs in ventilator-induced lung injury. *Am J Respir Cell Mol Biol* 2008;39:53–60.
8. Vaneker M, Joosten LA, Heunks LM, Snijdelaar DG, Halbertsma FJ, van Egmond J, Netea MG, van der Hoeven JG, Scheffer GJ. Low-tidal-volume mechanical ventilation induces a Toll-like receptor 4–dependent inflammatory response in healthy mice. *Anesthesiology* 2008;109:465–472.
9. Li H, Su X, Yan X, Wasserloos K, Chao W, Kaynar AM, Liu ZQ, Leikauf GD, Pitt BR, Zhang LM. Toll-like receptor 4–myeloid differentiation factor 88 signaling contributes to ventilator-induced lung injury in mice. *Anesthesiology* 2010;113:619–629.
10. Papaiahgari S, Yerrapureddy A, Reddy SR, Reddy NM, Dodd OJ, Crow MT, Grigoryev DN, Barnes K, Tuder RM, Yamamoto M, *et al*. Genetic and pharmacologic evidence links oxidative stress to ventilator-induced lung injury in mice. *Am J Respir Crit Care Med* 2007;176:1222–1235.
11. Peng X, Abdulnour RE, Sammani S, Ma SF, Han EJ, Hasan EJ, Tuder R, Garcia JG, Hassoun PM. Inducible nitric oxide synthase contributes to ventilator-induced lung injury. *Am J Respir Crit Care Med* 2005;172:470–479.
12. Takenaka K, Nishimura Y, Nishiuma T, Sakashita A, Yamashita T, Kobayashi K, Satouchi M, Ishida T, Kawashima S, Yokoyama M. Ventilator-induced lung injury is reduced in transgenic mice that overexpress endothelial nitric oxide synthase. *Am J Physiol Lung Cell Mol Physiol* 2006;290:L1078–L1086.
13. Jenkins RG, Su X, Su G, Scotton CJ, Camerer E, Laurent GJ, Davis GE, Chambers RC, Matthay MA, Sheppard D. Ligation of protease-activated receptor 1 enhances alpha(v)beta6 integrin–dependent TGF-beta activation and promotes acute lung injury. *J Clin Invest* 2006;116:1606–1614.
14. Li LF, Liao SK, Ko YS, Lee CH, Quinn DA. Hyperoxia increases ventilator-induced lung injury via mitogen-activated protein kinases: a prospective, controlled animal experiment. *Crit Care* 2007;11:R25.
15. Eckle T, Fullbier L, Wehrmann M, Khoury J, Mittelbronn M, Ibla J, Rosenberger P, Eltzschig HK. Identification of ectonucleotidases CD39 and CD73 in innate protection during acute lung injury. *J Immunol* 2007;178:8127–8137.
16. Bishai JM, Mitzner W, Tankersley CG, Wagner EM. PEEP-induced changes in epithelial permeability in inbred mouse strains. *Respir Physiol Neurobiol* 2007;156:340–344.
17. Yoshikawa S, King JA, Lausch RN, Penton AM, Eyal FG, Parker JC. Acute ventilator-induced vascular permeability and cytokine responses in isolated and *in situ* mouse lungs. *J Appl Physiol* 2004;97:2190–2199.
18. Leikauf GD, Concel VJ, Liu P, Bein K, Berndt A, Ganguly K, Jang AS, Brant KA, Dietsch M, Pope-Varsalona H, *et al*. Haplotype association mapping of acute lung injury in mice implicates activin A receptor, type 1. *Am J Respir Crit Care Med* 2011;183:1499–1509.

19. Peters LL, Robledo RF, Bult CJ, Churchill GA, Paigen BJ, Svenson KL. The mouse as a model for human biology: a resource guide for complex trait analysis. *Nat Rev Genet* 2007;8:58–69.
20. Leikauf GD, Pope-Varsalona H, Concel VJ, Liu P, Bein K, Berndt A, Martin TM, Ganguly K, Jang AS, Brant KA, *et al*. Integrative assessment of chlorine-induced acute lung injury in mice. *Am J Respir Cell Mol Biol* (In press)
21. Sodhi CP, Shi XH, Richardson WM, Grant ZS, Shapiro RA, Prindle T Jr, Branca M, Russo A, Gribar SC, Ma C, *et al*. Toll-like receptor-4 inhibits enterocyte proliferation via impaired beta-catenin signaling in necrotizing enterocolitis. *Gastroenterology* 2010;138:185–196.
22. Horng T, Medzhitov R. *Drosophila* MyD88 is an adapter in the Toll signaling pathway. *Proc Natl Acad Sci USA* 2001;98:12654–12658.
23. Moore KJ, Andersson LP, Ingalls RR, Monks BG, Li R, Arnaout MA, Golenbock DT, Freeman MW. Divergent response to LPS and bacteria in CD14-deficient murine macrophages. *J Immunol* 2000;165: 4272–4280.
24. Hoebe K, Du X, Georgel P, Janssen E, Tabeta K, Kim SO, Goode J, Lin P, Mann N, Mudd S, *et al*. Identification of Lps2 as a key transducer of MyD88-independent TIR signalling. *Nature* 2003;424:743–748.
25. Dickson SP, Wang K, Krantz I, Hakonarson H, Goldstein DB. Rare variants create synthetic genome-wide associations. *PLoS Biol* 2010;8: e1000294.
26. Keane TM, Goodstadt L, Danecek P, White MA, Wong K, Yalcin B, Heger A, Agam A, Slater G, Goodson M, *et al*. Mouse genomic variation and its effect on phenotypes and gene regulation. *Nature* 2011;477:289–294.
27. Villar J, Cabrera NE, Casula M, Valladares F, Flores C, Lopez-Aguilar J, Blanch L, Zhang H, Kacmarek RM, Slutsky AS. WNT/beta-catenin signaling is modulated by mechanical ventilation in an experimental model of acute lung injury. *Intensive Care Med* 2011;37:1201–1209.
28. Villar J, Cabrera NE, Valladares F, Casula M, Flores C, Blanch L, Quilez ME, Santana-Rodriguez N, Kacmarek RM, Slutsky AS. Activation of the Wnt/beta-catenin signaling pathway by mechanical ventilation is associated with ventilator-induced pulmonary fibrosis in healthy lungs. *PLoS ONE* 2011;6:e23914.
29. Flozak AS, Lam AP, Russell S, Jain M, Peled ON, Sheppard KA, Beri R, Mutlu GM, Budinger GR, Gottardi CJ. Beta-catenin/T-cell factor signaling is activated during lung injury and promotes the survival and migration of alveolar epithelial cells. *J Biol Chem* 2010;285:3157–3167.
30. Al Alam D, Green M, Tabatabai Irani R, Parsa S, Danopoulos S, Sala FG, Branch J, El Agha E, Tiozzo C, Voswinckel R, *et al*. Contrasting expression of canonical Wnt signaling reporters TOPGAL, BATGAL and Axin2(LacZ) during murine lung development and repair. *PLoS ONE* 2011;6:e23139.
31. Heise RL, Stober V, Cheluvaraju C, Hollingsworth JW, Garantziotis S. Mechanical stretch induces epithelial–mesenchymal transition in alveolar epithelia via hyaluronan activation of innate immunity. *J Biol Chem* 2011;286:17435–17444.
32. Königshoff M, Kramer M, Balsara N, Wilhelm J, Amarie OV, Jahn A, Rose F, Fink L, Seeger W, Schaefer L, *et al*. WNT1-inducible signaling protein-1 mediates pulmonary fibrosis in mice and is upregulated in humans with idiopathic pulmonary fibrosis. *J Clin Invest* 2009; 119:772–787.
33. Hu G, Malik AB, Minshall RD. Toll-like receptor 4 mediates neutrophil sequestration and lung injury induced by endotoxin and hyperinflation. *Crit Care Med* 2010;38:194–201.
34. Donaldson JG, Jackson CL. ARF family G proteins and their regulators: roles in membrane transport, development and disease. *Nat Rev Mol Cell Biol* 2011;12:362–375.
35. Dessauer CW. Adenylyl cyclase-A-kinase anchoring protein complexes: the next dimension in cAMP signaling. *Mol Pharmacol* 2009;76:935–941.
36. Berschneider B, Konigshoff M. WNT1 inducible signaling pathway protein 1 (WISP1): a novel mediator linking development and disease. *Int J Biochem Cell Biol* 2011;43:306–309.
37. Melotte V, Qu X, Ongenaert M, van Criekinge W, de Bruine AP, Baldwin HS, van Engeland M. The N-myc downstream regulated gene (NDRG) family: diverse functions, multiple applications. *FASEB J* 2010; 24:4153–4166.
38. Yoo BK, Gredler R, Chen D, Santhekadur PK, Fisher PB, Sarkar D. c-Met activation through a novel pathway involving osteopontin mediates oncogenesis by the transcription factor LSF. *J Hepatol* 2011; 55:1317–1324.
39. Porta-de-la-Riva M, Stanisavljevic J, Curto J, Franci C, Diaz VM, Garcia de Herreros A, Baulida J. TFCP2c/LSF/LBP-1c is required for Snail1-induced fibronectin gene expression. *Biochem J* 2011;435:563–568.
40. Santhekadur PK, Gredler R, Chen D, Siddiq A, Shen XN, Das SK, Emdad L, Fisher PB, Sarkar D. Late SV40 factor (LSF) enhances angiogenesis by transcriptionally up-regulating matrix metalloproteinase-9 (MMP-9). *J Biol Chem* 2012;287:3425–3432.
41. Kim JH, Suk MH, Yoon DW, Lee SH, Hur GY, Jung KH, Jeong HC, Lee SY, Suh IB, Shin C, *et al*. Inhibition of matrix metalloproteinase-9 prevents neutrophilic inflammation in ventilator-induced lung injury. *Am J Physiol Lung Cell Mol Physiol* 2006;291:L580–L587.
42. Albaiceta GM, Gutierrez-Fernandez A, Parra D, Astudillo A, Garcia-Prieto E, Taboada F, Fueyo A. Lack of matrix metalloproteinase-9 worsens ventilator-induced lung injury. *Am J Physiol Lung Cell Mol Physiol* 2008;294:L535–L543.
43. Jun JI, Lau LF. Taking aim at the extracellular matrix: CCN proteins as emerging therapeutic targets. *Nat Rev Drug Discov* 2011;10:945–963.
44. Cabrera-Benitez NE, Parotto M, Post M, Han B, Spieth PM, Cheng WE, Valladares F, Villar J, Liu M, Sato M, *et al*. Mechanical stress induces lung fibrosis by epithelial–mesenchymal transition. *Crit Care Med* 2012;40:510–517.
45. Opitz B, van Laak V, Eitel J, Suttorp N. Innate immune recognition in infectious and noninfectious diseases of the lung. *Am J Respir Crit Care Med* 2010;181:1294–1309.
46. da Silva Correia J, Ulevitch RJ. MD-2 and TLR4 N-linked glycosylations are important for a functional lipopolysaccharide receptor. *J Biol Chem* 2002;277:1845–1854.
47. Desnoyers L, Arnott D, Pennica D. WISP-1 binds to decorin and biglycan. *J Biol Chem* 2001;276:47599–47607.
48. Babelova A, Moreth K, Tsalastra-Greul W, Zeng-Brouwers J, Eickelberg O, Young MF, Bruckner P, Pfeilschifter J, Schaefer RM, Grone HJ, *et al*. Biglycan, a danger signal that activates the NLRP3 inflammasome via Toll-like and P2X receptors. *J Biol Chem* 2009;284: 24035–24048.
49. Moreth K, Iozzo RV, Schaefer L. Small leucine-rich proteoglycans orchestrate receptor crosstalk during inflammation. *Cell Cycle* 2012;11: 2084–2091.
50. Laplante P, Amireault P, Subang R, Dieude M, Levine JS, Rauch J. Interaction of beta2-glycoprotein I with lipopolysaccharide leads to Toll-like receptor 4 (TLR4)–dependent activation of macrophages. *J Biol Chem* 2011;286:42494–42503.